

Search for MSSM H^+ bosons decaying into $H^+ \rightarrow \tau^+ \nu_\tau$ and $H^+ \rightarrow t\bar{b}$ with $\ell + \tau(\rightarrow had)$ and dilepton final states

Pietro Vischia^{*†}

IST/LIP-Lisboa

E-mail: pietro.vischia@gmail.com

Results are presented of a search for a charged Higgs boson with a mass larger than the top quark in the $gg \rightarrow H^+ tb$ production process using 19.7 fb^{-1} of data collected in proton-proton collisions at $\sqrt{s} = 8 \text{ TeV}$ with the CMS detector. The final states considered contain either one electron and one muon, or two electrons, or two muons, or one muon plus one hadronically decaying tau lepton, corresponding to the charged Higgs decays $H^+ \rightarrow tb$ and $H^+ \rightarrow \tau^+ \nu$. The full production and decay chain includes $gg \rightarrow H^+ tb \rightarrow (\tau_h \nu)(\mu \nu b)b$ and $gg \rightarrow H^+ tb \rightarrow (\ell \nu b b)(\ell' \nu b)b$, with ℓ, ℓ' being an electron or a muon. We find no evidence for a charged Higgs signal and set upper limits on its production rate for mass values in the range 180-600 GeV.

*Prospects for Charged Higgs Discovery at Colliders - CHARGED 2014,
16-18 September 2014
Uppsala University, Sweden*

^{*}Speaker.

[†]On behalf of the CMS Collaboration

1. Introduction

The Higgs boson may be at the origin of the mechanism through which particles acquire mass. A new scalar boson was discovered by the CMS and ATLAS collaborations [1, 2] compatible with the standard model (SM) Higgs boson. In two-Higgs doublet models, such as the Minimal Supersymmetric extension of the SM (MSSM) [3], the Higgs sector contains five particles: three neutral (the CP-even h^0 and H^0 , the CP-odd A^0) and two charged (H^\pm) Higgs bosons. Whereas the neutral Higgs boson is compatible with both the SM and the MSSM, the detection of a charged Higgs boson would unequivocally point to new physics beyond the SM. If the charged Higgs boson mass is smaller than the top quark mass, stringent limits have already been set on its production directly through top quark decays on the branching fraction $B(t \rightarrow H^+b)$ at the level of 2–3% for charged Higgs boson masses between 80 and 160 GeV, by both the ATLAS and CMS collaborations [4, 5, 6, 7, 8].

A charged Higgs boson with mass larger than the top quark mass, instead, can be produced in association with a top quark through the process $gg \rightarrow H^+tb$ (Fig. 1). While at low charged Higgs boson masses the dominant decay mode in most MSSM models is $H^+ \rightarrow \tau^+ \nu_\tau$, for masses larger than the top quark mass the $H^+ \rightarrow t\bar{b}$ decay channel opens up, and quickly becomes dominant around $m_{H^+} = 200$ GeV. Charge conjugate processes are always implied throughout this document. The present document considers the decay chains $gg \rightarrow H^+tb \rightarrow (\tau_h \nu_\tau)(\mu \nu_\mu b)b$ and $gg \rightarrow H^+tb \rightarrow (\ell \nu_\ell bb)(\ell' \nu_{\ell'} b)b$ (ℓ and ℓ' being electrons or muons), with the charged Higgs decays $H^+ \rightarrow t\bar{b}$ and $H^+ \rightarrow \tau^+ \nu_\tau$. The $m_h^{\text{mod}+}$ scenario [9], with the choice of $\tan\beta = 30$, is chosen as benchmark scenario. The production cross section and theoretical branching fractions for the heavy charged Higgs have been evaluated by the LHC Higgs cross section working group [10], and are summarized in Ref. [11]. This document summarizes a CMS search for a charged Higgs boson with mass heavier than the top quark mass, $m_{H^+} > m_t$, performed using data from proton-proton collisions at the LHC at $\sqrt{s} = 8$ TeV, collected with the CMS detector. The search is described in detail in Ref. [11].

The main results presented here are independent of the specific MSSM scenario chosen for signal modeling. To simplify the presentation, for all plots and numbers of expected signal events we assume a cross section of 1 pb.

Depending on the charged Higgs boson decay, the final states studied include one muon plus one hadronically decaying tau lepton (labeled “ $\mu \tau_h$ ”), or two leptons ($e\mu$, ee , or $\mu\mu$, collectively labeled “dileptons”) In all final states, the presence of at least two jets, of which at least one is “b-tagged”, and missing transverse energy due to the neutrinos are also required. The search is performed with 19.7 fb^{-1} of data collected in proton-proton collisions at $\sqrt{s} = 8$ TeV with the CMS detector.

2. Signal and background Monte Carlo simulation

Simulated samples of SM processes are generated using the MADGRAPH 5.1.3.30 [12, 13], PYTHIA 6 [14] or POWHEG 1.0 [15] event generator programs. The MADGRAPH samples use the CTEQ6L1 PDF set, a renormalization scale equal to 91.1880 and a 20 GeV jet matching threshold for the K_T -MLM showering scheme. The POWHEG samples use the CTEQ6m PDF set.

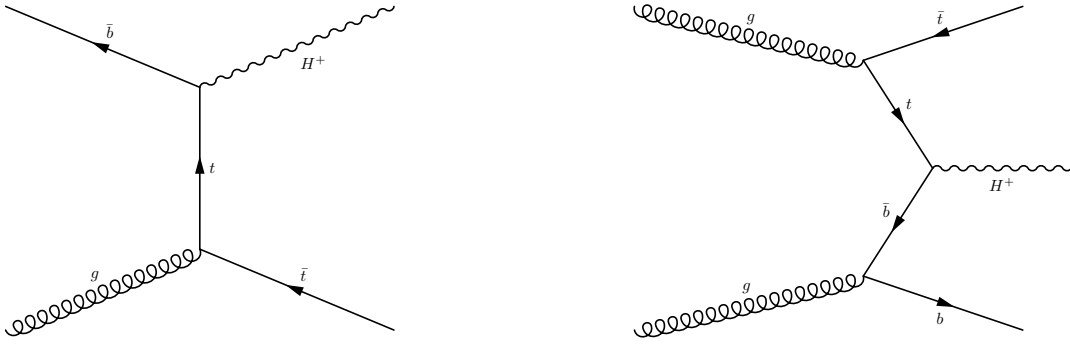


Figure 1: Feynman diagrams of the charged Higgs boson production in the MSSM scenario for a charged Higgs boson mass larger than the top quark mass, $m_{H^+} > m_t$.

The di-boson cross sections are based on MCFM [16] computations from [17]. Apart from the SM $t\bar{t}$ and MSSM charged Higgs processes, the relevant processes are from single top, vector boson (W/Z) and Drell-Yan (DY) production. QCD samples are also considered, since jets can be misidentified as leptons during the reconstruction process. Single top events are simulated with POWHEG, while MADGRAPH is used for $t\bar{t}$, W+jet, and DY events. All other samples (QCD and dibosons) use PYTHIA. For the signal events, the production of MSSM charged Higgs is generated with PYTHIA. The τ decays are simulated with TAUOLA [18] which correctly accounts for the τ lepton polarization in describing the decay kinematics.

For both signal and background events, multiple proton-proton interactions in the same or nearby bunch crossings (pileup) are simulated using PYTHIA and superimposed on the hard collision. The simulation of the detector response to new physics events is performed using the full CMS simulation. The CMS detector response is simulated with GEANT4 v. 9.3 Rev01 [19].

3. Object definition and event reconstruction

The data used for this search were collected using triggers with either one isolated muon with p_T threshold of 24 GeV, or with two leptons (one lepton with $p_T > 17$ GeV and the other with $p_T > 8$ GeV), for the $\mu\tau_h$ and dilepton ($e\mu$, ee , and $\mu\mu$) channels, respectively. Events are reconstructed using the particle-flow (PF) algorithm [20].

Electron candidates are reconstructed starting from a cluster of energy deposits in the electromagnetic calorimeter. The cluster is then matched to a reconstructed track. Shower shape and consistency between the cluster energy and the track momentum are then used for electron selection. Muon candidates are reconstructed by performing a global fit that requires consistent hit patterns in the tracker and the muon system. Leptons are required to be isolated from other activity in the event. A measure of lepton isolation I_{rel} is the scalar sum of the p_T of all PF particles, excluding the lepton, divided by the lepton p_T , within a cone of radius $\Delta R = \sqrt{(\Delta\eta)^2 + (\Delta\phi)^2} = 0.4$, where $\Delta\eta$ ($\Delta\phi$) is the difference in η (ϕ) between the lepton and the PF particle at the vertex.

Hadronic τ decays are reconstructed with the hadron-plus-strips (HPS) algorithm [21]. Tracking and calorimeter information are used by analyzing the constituents of jets in order to identify

specific τ decay modes, by taking full advantage of the performance provided by PF techniques for reconstructing individual charged hadrons and photons. Additional requirements are applied to discriminate genuine τ leptons from prompt electrons and muons. The τ charge is taken as the sum of the charges of the charged hadrons (prongs) in the signal cone. The τ reconstruction efficiency of this algorithm is estimated to be approximately 60% (i.e. “medium” working point in Ref. [21]) for $p_T^\tau > 20$ GeV, corresponding to a probability of approximately 0.5% for generic hadronic jets to be misidentified as τ_h .

Jets are reconstructed from all the PF particles using the anti- k_T clustering algorithm [22] with a distance parameter of 0.5, as implemented in the FASTJET package [23]. Corrections aimed to mitigating the effect of pileup on the jet reconstruction are applied [23]. At least one (or two, for the dilepton final states) of these jets must be consistent with containing the decay of a heavy-flavor hadron, as identified using the “medium” operating point of the combined secondary vertex b-tagging algorithm (CSVM) [24]. We refer to such jets as “b-tagged jets”.

The missing transverse energy (E_T^{miss}) is defined as the magnitude of the negative vector sum of the transverse momenta of all PF particles over the full calorimeter coverage ($|\eta| < 5$). Calibrations applied to the energy measurements of jets are propagated consistently as a correction to the E_T^{miss} .

4. Hadronic τ decays: the $\mu\tau_h$ final state

The event selection used is similar to that used in the measurement of the top quark pair production cross section in dilepton final states containing a τ [25, 26], with the purpose of minimizing the contribution from non-irreducible SM backgrounds. A single-muon trigger with a threshold of 24 GeV is used to select the events.

The events are selected by requiring one isolated ($I_{\text{rel}} < 0.12$) muon with $p_T > 30$ GeV and $|\eta| < 2.1$. The event must contain one hadronically decaying τ , i.e. τ_h , with $p_T > 20$ GeV within $|\eta| < 2.4$, at least two jets with $p_T > 30$ GeV within $|\eta| < 2.4$, with at least one jet identified as originating from the hadronization of a b quark, and $E_T^{\text{miss}} > 40$ GeV. The τ_h and the muon are required to have opposite electric charges. The muon is required to be separated from any selected jet by a distance $\Delta R > 0.4$. Events with an additional electron (muon) with $I_{\text{rel}} < 0.2$ and $p_T > 15$ (10) GeV are rejected.

The backgrounds arise from two sources, the first with misidentified τ_h from generic jets, which is estimated from data, and the second with genuine τ_h (or from other remaining sources), which is estimated from simulation. The background due to Drell-Yan or $t\bar{t}$ events with one electron or muon misidentified as a τ_h is small and it is estimated from simulation, and it is also included in the second category.

The misidentified τ_h background dominant contribution comes from W +jets, and from $t\bar{t} \rightarrow W^+W^-b\bar{b} \rightarrow \mu\nu q\bar{q}'b\bar{b}$ events. This contribution is estimated from data using the procedure described in Ref. [4], improved by taking into account the quark and gluon jets compositions (evaluated from simulation) of the samples used throughout the procedure.

The backgrounds with genuine τ leptons are estimated from simulation.

Data and the simulated event yield at various stages of the event selection are shown in Fig. 2, *right*. The backgrounds are normalized to the SM prediction obtained from the simulation. A

good agreement is found between data and the SM background. The expected event yields in the presence of $H^+ \rightarrow tb$ and $H^+ \rightarrow \tau^+ \nu_\tau$ decays are shown as dashed lines for $m_{H^+} = 250$ GeV.

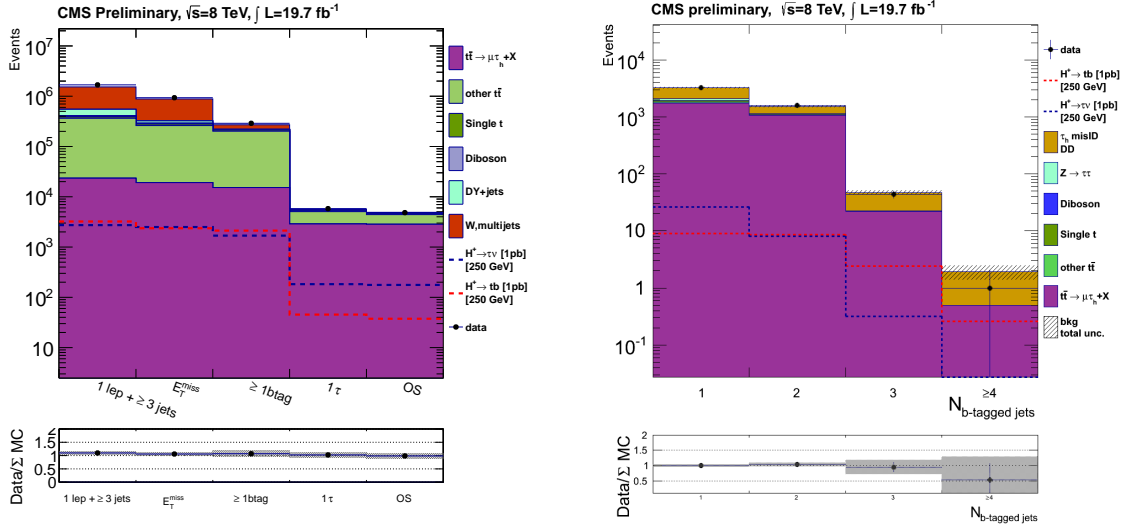


Figure 2: *Left:* Event yields after each selection step, where OS indicates the requirement to have opposite electric charges for a τ_h and a μ . The backgrounds are estimated from simulation and normalized to the standard model prediction. *Right:* the b -tagged jet multiplicity after the full event selection for data (points) and for SM backgrounds, are shown together with the signal expectations for the MSSM charged Higgs boson mass $m_{H^\pm} = 250$ GeV. The “misidentified τ_h ” component is estimated using the data-driven method, while the remaining simulated background contributions are normalized to the SM predicted values. The expected event yield in the presence of the $H^+ \rightarrow tb$ and $H^+ \rightarrow \tau^+ \nu_\tau$ decays is shown as dashed lines for $m_{H^+} = 250$ GeV. The charged Higgs signal yields are shown assuming a cross section of 1 pb and a branching fraction $B = 100\%$ for each decay channel. The bottom panel shows the ratios of data over the sum of the SM backgrounds with the total uncertainties. Statistical and systematic uncertainties are added in quadrature.

The b -tagged jet multiplicity is shown after the full event selection in Fig. 2, *right*. The ratio of the data to the sum of expected SM background contributions are shown in the bottom panel of each of the figures.

4.1 Systematic uncertainties

The main sources of systematic uncertainties are due to tau identification, jet energy scale (JES), jet energy resolution (JER), E_T^{miss} scale, and to the estimate of the tau misidentification (“tau-fake”) background (from data). The evaluation of the systematic uncertainty on tau-fake background ($\epsilon_{\tau\text{-fakes}}$) is discussed in the previous section.

All systematic uncertainties for signal and background events are summarized in Table 1.

4.2 Results

The number of expected events for the SM backgrounds, the number of signal events from $gg \rightarrow H^\pm tb$ processes for $m_{H^\pm} = 250$ GeV for the decay modes $H^\pm \rightarrow tb$ and $H^\pm \rightarrow \tau_h \nu$, and the

Table 1: The systematic uncertainties for the $\mu\tau_h$ final state (in %) for backgrounds, and for signal events from $gg \rightarrow H^\pm tb$ processes for $m_{H^\pm}=250$ GeV. The uncertainties marked with “shape” depend only on the b-tagged jets multiplicity distribution bin. These systematic uncertainties are given as the input to the exclusion limit calculation.

	Signal	$t\bar{t}\ell\tau$	$t\bar{t}\ell\ell$	τ fakes	Single top	VV	DY($ee,\mu\mu$)	DY($\tau\tau$)
τ -jet id	6	6			6	6		6
jet, $\ell \rightarrow \tau$ mis-id			30				30	
JES+JER+ E_T^{miss} +TES	6	5	4		6	11	100	21
b-jet tagging	6	5	5		7			
jet \rightarrow b mis-id						9	9	9
pile up	4	2	8		2	3	25	4
lepton selection	2	2	2		2	2	2	2
τ fakes				11				
cross section	30	3	3		8	4	4	
top quark p_T scale		shape	shape					
τ embedding								shape
matching scale		1	1					
PDF	1	5	5					
Q^2 scale		3	3					
MC statistics	3	1	3		4	11	100	35
luminosity					3			

number of observed events after all selection cuts are summarized in Table 2. The misidentified τ_h background measured from data, 1544 ± 175 (stat. + syst.) events, is consistent with the expectations from simulation. The statistical and systematic uncertainties evaluated as described in Section 4.1 are also shown. The number of signal events are shown assuming a cross section of 1 pb and 100% branching fraction for each decay mode.

5. Dileptons: the $e\mu$, ee , $\mu\mu$ final states

As the $H^\pm \rightarrow tb$ decay is the dominant decay mode for masses larger than $m_{H^\pm} = 200$ GeV, the dilepton ($e\mu$, ee , $\mu\mu$) final states are important probes to search for charged Higgs masses above this mass range. Through the production mechanism $gg \rightarrow tH^\pm(b)$ and the subsequent charged Higgs decay mode, the final states include two top quarks together with one or two additional b-quarks. Here, the $e\mu$, ee , and $\mu\mu$ dilepton final states are studied, where the full production and decay chain goes through $gg \rightarrow H^\pm t(b) \rightarrow (\ell\nu_\ell bb)(\ell'\nu_{\ell'} b)(b)$, where ℓ and ℓ' can be either electrons or muons. These final states are similar to the SM $t\bar{t}$ dilepton final states, with the addition of one (or two) b -jets.

5.1 Event selection and yields

The event selection is similar to the one described in Ref. [27], aiming at reducing the contribution from SM backgrounds other than from $t\bar{t}$. Data are collected with double-lepton triggers

Table 2: Number of expected events in the $\mu\tau_h$ final state for the SM backgrounds and in the presence of a charged Higgs boson signal from $H^+ \rightarrow tb$ and $H^+ \rightarrow \tau^+\nu_\tau$ decays for $m_{H^+} = 250$ GeV are shown together with the number of observed events after the final event selection. The charged Higgs signal is shown assuming a cross section of 1 pb and a branching fraction $B = 100\%$ for each decay channel.

Source	$N_{\text{events}} (\pm \text{stat.} \pm \text{syst.})$
$H^+ \rightarrow \tau_h\nu, M_{H^+} = 250$ GeV	$176 \pm 6 \pm 13$
$H^+ \rightarrow tb, M_{H^+} = 250$ GeV	$37 \pm 2 \pm 3$
$t\bar{t} \rightarrow \mu\tau_h + X$	$2836 \pm 42 \pm 237$
τ fakes	1544 ± 175
$t\bar{t}$ dileptons	$96 \pm 7 \pm 13$
$Z/\gamma \rightarrow ee, \mu\mu$	$12 \pm 5 \pm 4$
$Z/\gamma \rightarrow \tau\tau$	$162 \pm 20 \pm 14$
single top	$150 \pm 8 \pm 18$
dibosons	$20 \pm 1 \pm 2$
Total expected	$4821 \pm 48 \pm 296$
Data	4839

(one electron and one muon, or two electrons, or two muons) with p_T thresholds of 17 GeV for one lepton and 8 GeV for the other. The dilepton trigger efficiency is corrected by a multiplicative data-to-simulation scale factor dependent on the final state, in order to provide agreement between data and simulation.

After offline reconstruction, events are selected with two isolated, oppositely charged, leptons (one electron and one muon, or two electrons, or two muons) with $p_T > 20$ GeV and $|\eta| < 2.5$ ($|\eta| < 2.4$) for electrons (muons), and at least two jets with $p_T > 30$ GeV and $|\eta| < 2.4$. It is required that the isolation is $(I_{\text{photon}} + I_{\text{ch.hadron}} + I_{\text{neut.hadron}})/p_T < 0.15$. The data-to-simulation scale factors for the trigger and lepton identification and isolation efficiencies are of the order of 1%, and a 2% uncertainty is found appropriate for describing the overall uncertainty on the event yields due to the identification, isolation and trigger efficiencies.

Jets are further required not to overlap within a cone of $\Delta R < 0.4$ with the isolated leptons. A minimum dilepton invariant mass of 12 GeV is required to reject SM background from low mass resonances. This requirement has no impact on the signal selection. A minimum requirement is made on the reconstructed missing transverse energy, i.e. $E_T^{\text{miss}} > 40$ GeV. Since four b -jets are expected in the final state, at least two b -tagged jets are required in the events.

The number of data events after each selection cut are compared to expectations from SM backgrounds, and are shown in Fig. 3, *left*. The results are in good agreement with SM background expectations.

The b -tagged jet multiplicity distribution for all the dilepton final states is shown after the full event selection in Fig. 3, *right*. A good agreement between data and the sum of the expected backgrounds is found for both cases.

5.2 Systematic uncertainties

The main sources of systematic uncertainties are due to jet energy scale (JES), jet energy

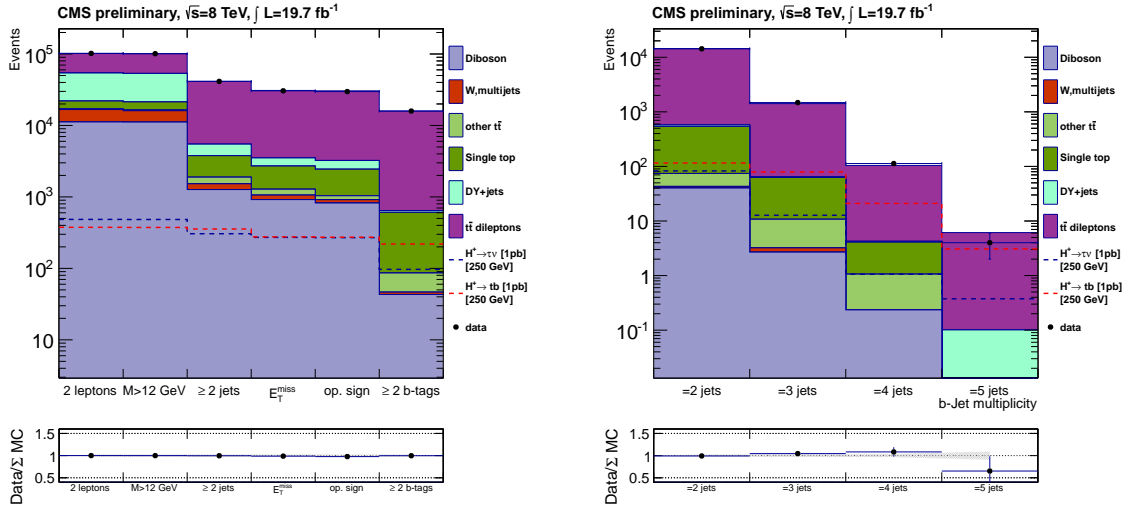


Figure 3: *Left:* event yields at different selection cut levels for the representative $e\mu$ final state. *Right:* the b -tagged jet multiplicity after the full event selection for data (points) and for SM background expectations, in the $e\mu$ final state. The simulated background contributions are normalized to the SM predicted values. Expectations for the MSSM charged Higgs boson for $m_{H^\pm} = 250$ GeV, for the $H^\pm \rightarrow tb$ and $H^\pm \rightarrow \tau_h \nu$ decays, are also shown. The hatched region shows the estimated total uncertainty associated with the luminosity acquired. The bottom panel shows the ratios of data over the sum of the SM backgrounds with the statistical uncertainty.

resolution (JER) and E_T^{miss} scale, and to the b -tagging uncertainty. All systematic uncertainties for signal and background events are summarized in Table 3.

5.3 Results

The number of expected events after all selection cuts in the dilepton final states are summarized in Table 4 for the SM background processes and for a charged Higgs boson with a mass of $m_{H^\pm} = 250$ GeV. Statistical and systematic uncertainties evaluated as described in Section 4 are also shown.

6. Limits

An excess of events in the $\mu\tau_h$ and dilepton ($e\mu$, ee and $\mu\mu$) final states, is expected in the presence of the charged Higgs. A CL_s method [28] is used in order to obtain the upper limit at 95% C.L. on the excess of the events in addition to the expected SM background. The b -tagged jet multiplicity distributions shown in Fig 3, *right*, and Fig. 3, *right*, are used in a binned maximum-likelihood fit in order to extract a possible signal. Both statistical and systematic uncertainties are propagated to the limits by including the corresponding shapes of the b -jet multiplicity distribution calculated with up and down variations ($\pm 1\sigma$) separately for each component, and then feeding those distributions to the limit calculations. An upper limit on $\sigma \times B$ (in pb) is estimated.

The branching ratios for $H^+ \rightarrow \tau^+ \nu_\tau$ and $H^+ \rightarrow t\bar{b}$ from the reference scenario are first used to derive model dependent upper limits on the cross section times branching fraction. The results of

Table 3: The systematic uncertainties (in %) for backgrounds, and for signal events for the dilepton channels for a charged Higgs boson mass $m_{H^\pm}=250$ GeV. The uncertainties marked with “shape” depend only on the b-tagged jets multiplicity distribution bin. These systematic uncertainties are given as the input to the exclusion limit calculation.

	Signal	$t\bar{t}$	DY	W+jets	Single top	VV
Energy scales (JES+JER+ E_T^{miss})	2	2	6	11	4	7
b-jet tagging	3	4	9	10	4	9
jet \rightarrow b mis-id	3	4	10	11	4	9
pile up	5	5	6	4	6	6
dilepton selection	3	3	3	3	3	3
cross section	30	3	4	5	7	4
DY E_T^{miss} modeling			30			
top quark p_T scale		shape				
matching scale		1				
PDF	1	5				
Q^2 scale		3				
MC statistics	1	1	7	43	2	4
luminosity	3					

Table 4: Number of expected events for the SM backgrounds and for signal events with a charged Higgs mass of $m_{H^\pm}=250$ GeV in the $e\mu$, ee , and $\mu\mu$ dilepton final states after the final event selection. The charged Higgs signal is shown assuming a cross section of 1 pb and a branching fraction $B = 100\%$ for each decay channel. Event yields are corrected with the trigger and selection efficiencies. Statistical and systematic uncertainties are shown.

Channel	ee	$e\mu$	$\mu\mu$
$H^+ \rightarrow \tau\nu, M_{H^+} = 250$ GeV	$39 \pm 3 \pm 3$	$97 \pm 4 \pm 5$	$40 \pm 3 \pm 3$
$H^+ \rightarrow tb, M_{H^+} = 250$ GeV	$85 \pm 3 \pm 2$	$219 \pm 5 \pm 5$	$90 \pm 3 \pm 2$
$t\bar{t}$ dileptons	$5693 \pm 17 \pm 140$	$15295 \pm 28 \pm 376$	$6333 \pm 18 \pm 156$
other $t\bar{t}$	$22 \pm 4 \pm 1$	$40 \pm 5 \pm 1$	$16 \pm 3 \pm 0$
Drell-Yan	$96 \pm 8 \pm 2$	$38 \pm 3 \pm 1$	$138 \pm 10 \pm 4$
W+jets, multi-jets	$6 \pm 2 \pm 0$	$4 \pm 1 \pm 0$	$0 \pm 1 \pm 0$
single top	$198 \pm 6 \pm 5$	$522 \pm 16 \pm 13$	$228 \pm 10 \pm 6$
dibosons	$15 \pm 1 \pm 0$	$43 \pm 2 \pm 1$	$20 \pm 1 \pm 1$
total SM backgrounds	$6030 \pm 20 \pm 140$	$15942 \pm 33 \pm 376$	$6735 \pm 23 \pm 156$
data	6162	15902	6955

the limit computation are shown for the combination of the $e\mu$, ee , $\mu\mu$, and $\mu\tau$ final states in Fig. 4; the excluded values of $\sigma \times B$ are roughly two orders of magnitude larger than those predicted by the reference scenario.

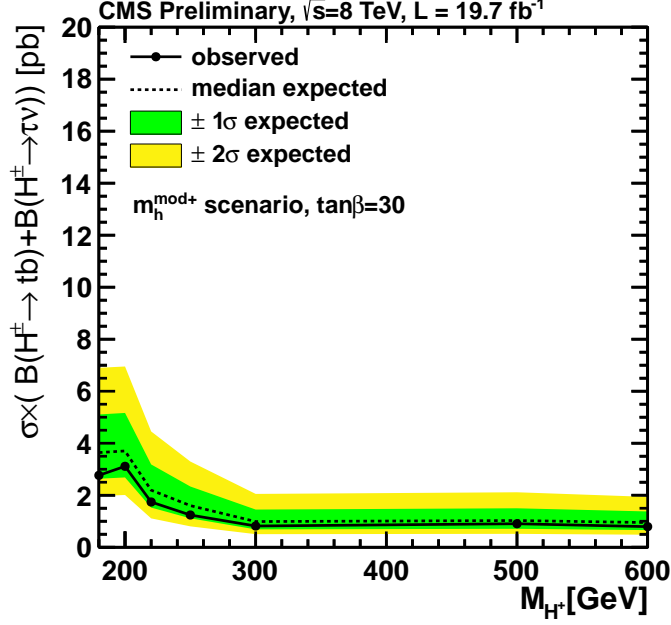


Figure 4: The 95% confidence level exclusion limits estimated from the combination of the $\mu\tau_h$, $e\mu$, ee , and $\mu\mu$ final states, when imposing the branching ratios for the two decay channels to be the ones predicted by the $m_h^{\text{mod}+}$ MSSM scenario.

Finally, the assumption that only either one of the decay modes is contributing to the given final state is made. The results of such an approach is shown in Fig. 5. In order to check for biases in the limit setting procedure, a signal injection test has been performed by injecting a known signal of different strengths into the estimated background. The results confirmed that the limit setting procedure is unbiased.

7. Conclusions

A direct search for the charged Higgs boson with a mass larger than the top quark mass, produced via $gg \rightarrow H^+ t(b)$, with decays $H^+ \rightarrow tb$ and $H^+ \rightarrow \tau_h \nu$, has been presented. The search has been performed in the $\mu\tau_h$, $e\mu$, ee , and $\mu\mu$ dilepton final states, with the full 2012 dataset of 19.7 fb^{-1} of data from proton-proton collisions at $\sqrt{s} = 8 \text{ TeV}$ collected using the CMS detector.

In both final states, the dominant SM background contribution comes from $t\bar{t}$ events: from the irreducible $t\bar{t}$ “tau dilepton” channel for the former, and from the $t\bar{t}$ dilepton events for the latter. An additional background in the $\mu\tau_h$ final state comes from events in which one jet is misidentified as the τ jet. No significant excess of events in data is found with respect to expectations. The number of candidate events found are in agreement with the expected SM event yields.

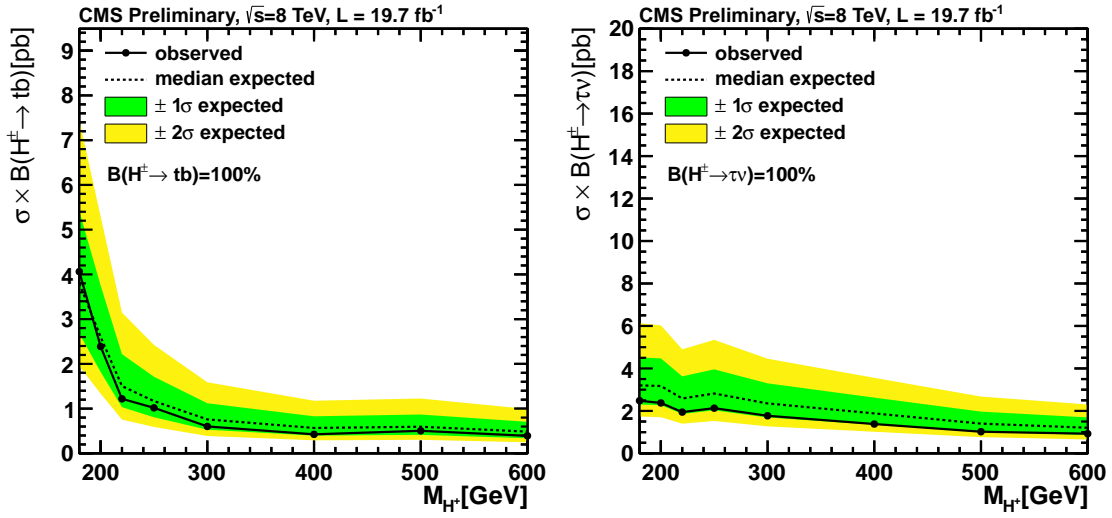


Figure 5: The 95% confidence level exclusion limits estimated from the combination of the $\mu\tau_h$, $e\mu$, ee , and $\mu\mu$ final states when assuming $B(H^+ \rightarrow t\bar{b}) = 100\%$ (left) and $B(H^+ \rightarrow \tau^+\nu_\tau) = 100\%$ (right). The $\pm 1\sigma$ and $\pm 2\sigma$ bands around the expected limits are also shown.

Upper limits on the cross section times branching fraction for the two decay channels, $B(H^+ \rightarrow t\bar{b})$ and $B(H^+ \rightarrow \tau_h\nu)$, are computed by separately setting to 100% the branching fraction for one channel and to 0% the branching fraction for the other one, respectively. The 95% CL limits are set to $\sigma \times B(H^+ \rightarrow t\bar{b}) \simeq 1 - 2$ pb and $\sigma \times B(H^+ \rightarrow \tau_h\nu) \simeq 4 - 5$ pb for masses between 180 and 600 GeV.

References

- [1] S. Chatrchyan *et al.*, “Observation of a new boson at a mass of 125 GeV with the CMS experiment at the LHC,” *Phys. Lett. B*, vol. 716, pp. 30–61, 2012.
- [2] G. Aad *et al.*, “Observation of a new particle in the search for the standard model Higgs boson with the ATLAS detector at the LHC,” *Phys. Lett. B*, vol. 716, pp. 1–29, 2012.
- [3] S. P. Martin, “A Supersymmetry Primer,” 1997.
- [4] S. Chatrchyan *et al.*, “Updated search for a light charged Higgs boson in top quark decays in pp collisions at $\sqrt{s} = 7$ TeV,” CMS Physics Analysis Summary CMS-PAS-HIG-12-052, 2012.
- [5] G. Aad *et al.*, “Search for charged Higgs bosons through the violation of lepton universality in $t\bar{t}$ events using pp collision data at $\sqrt{s} = 7$ TeV with the ATLAS experiment,” *JHEP*, vol. 03, p. 076, 2013.
- [6] S. Chatrchyan *et al.*, “Search for a light charged Higgs boson in top quark decays in pp collisions at $\sqrt{s} = 7$ TeV,” *JHEP*, vol. 07, p. 143, 2012.
- [7] G. Aad *et al.*, “Search for charged Higgs bosons decaying via $H^+ \rightarrow \tau\nu$ in top quark pair events using pp collision data at $\sqrt{s} = 7$ TeV with the ATLAS detector,” *JHEP*, vol. 06, p. 039, 2012.
- [8] G. Aad *et al.*, “Search for a light charged Higgs boson in the decay channel $H^+ \rightarrow c\bar{s}$ in $t\bar{t}$ events using pp collisions at $\sqrt{s} = 7$ TeV with the ATLAS detector,” *Eur. Phys. J. C*, vol. 73, p. 2465, 2013.

- [9] M. Carena, S. Heinemeyer, O. Stal, C. Wagner, and G. Weiglein, “MSSM Higgs Boson Searches at the LHC: Benchmark Scenarios after the Discovery of a Higgs-like Particle,” *Eur. Phys. J. C*, vol. 73, p. 2552, 2013.
- [10] LHC Cross sections working group. <https://twiki.cern.ch/twiki/bin/view/LHCPhysics/LHCHXSWG>.
- [11] “Search for a heavy charged Higgs boson in proton-proton collisions at $\sqrt{s}=8$ TeV with the CMS detector,” Tech. Rep. CMS-PAS-HIG-13-026, CERN, Geneva, 2014.
- [12] J. Alwall, R. Frederix, S. Frixione, V. Hirschi, F. Maltoni, *et al.*, “The automated computation of tree-level and next-to-leading order differential cross sections, and their matching to parton shower simulations,” *JHEP*, vol. 07, p. 079, 2014.
- [13] J. Alwall, M. Herquet, F. Maltoni, O. Mattelaer, and T. Stelzer, “MadGraph 5 : Going Beyond,” *JHEP*, vol. 06, p. 128, 2011.
- [14] T. Sjöstrand, S. Mrenna, and P. Z. Skands, “PYTHIA 6.4 Physics and Manual,” *JHEP*, vol. 05, p. 026, 2006.
- [15] S. Alioli, P. Nason, C. Oleari, and E. Re, “A general framework for implementing NLO calculations in shower Monte Carlo programs: the POWHEG BOX,” *JHEP*, vol. 06, p. 043, 2010.
- [16] C. W. John M. Campbell, R. Keith Ellis, “Vector boson pair production at the LHC,” *JHEP*, vol. 07, p. 018, 2011.
- [17] J. M. Campbell, R. K. Ellis, and C. Williams, “Vector boson pair production at the LHC,” *JHEP*, vol. 07, p. 018, 2011.
- [18] Z. Was, “TAUOLA the library for tau lepton decay, and KKMC / KORALB / KORALZ status report,” *Nucl. Phys. Proc. Suppl.*, vol. 98, p. 96, 2001.
- [19] S. Agostinelli *et al.*, “GEANT4: A simulation toolkit,” *Nucl. Instrum. Meth.*, vol. A506, pp. 250–303, 2003.
- [20] CMS, “Commissioning of the particle flow reconstruction in minimum-bias and jet events from pp collisions at 7 TeV,” CMS Physics Analysis Summary CMS-PAS-PFT-10-002, 2010.
- [21] CMS, “Performance of tau lepton reconstruction and identification in CMS,” *JINST*, vol. 7, p. P01001, 2012.
- [22] M. Cacciari, G. P. Salam, and G. Soyez, “The anti- k_T jet clustering algorithm,” *JHEP*, vol. 04, p. 063, 2008.
- [23] M. Cacciari and G. Salam, “Pileup subtraction using jet areas,” *Phys. Lett. B*, vol. 659, pp. 119–126, 2008.
- [24] S. Chatrchyan *et al.*, “Identification of b-quark jets with the CMS experiment,” *JINST*, vol. 8, p. P04013, 2013.
- [25] S. Chatrchyan *et al.*, “Measurement of the top quark pair production cross section in pp collisions at $\sqrt{s} = 7$ TeV in dilepton final states containing a τ ,” *Phys. Rev. D*, vol. 85, p. 112007, 2012.
- [26] V. Khachatryan *et al.*, “Measurement of the $t\bar{t}$ production cross section in pp collisions at $\sqrt{s} = 8$ TeV in dilepton final states containing one τ lepton,” 2014.
- [27] S. Chatrchyan *et al.*, “Measurement of the $t\bar{t}$ production cross section in the dilepton channel in pp collisions at $\sqrt{s} = 7$ TeV,” *JHEP*, vol. 11, p. 067, 2012.
- [28] G. Cowan, K. Cranmer, E. Gross, and O. Vitells, “Asymptotic formulae for likelihood-based tests of new physics,” *Eur. Phys. J. C*, vol. 71, p. 1554, 2011.